J. Fluid Mech. (1966), *vol.* 24, *part* 2, *pp.* 293–306
Printed in Great Britain

Interfacial circulation due to surface-active agents in steady two-phase flows

By D. B. R. KENNING AND M. G. COOPER
Department of Engineering, University of Cambridge

(Received 5 April 1965 and in revised form 28 July 1965)

Steady circulatory motions at the surface of tap-water flowing in an open channel and past a hemispherical air bubble on a channel wall are described and explained by the presence of a film of surface-active material. Boundary conditions for the liquid phase are derived by assuming that the surface film is insoluble and incompressible. Good agreement is obtained between the theoretical and measured velocity fields in the open-channel flow.

1. Introduction

The presence of small amounts of adsorbed surface-active agent (surfactant) at the interface between two fluids in relative motion has been shown to have a pronounced effect on the transmission of shear stresses across the interface. For example, the inhibition by surfactants of internal circulation within bubbles and drops moving in uniform streams has been described by Frumkin & Levich (1947), Gardner & Skelland (1951), Gardner & Hale (1953), Griffith (1960, 1962) and others, who proposed the following explanation. Surface-active material is either steadily adsorbed at the front of the bubble or already present on the surface, forming a film of monomolecular thickness. Relative movement of the external bulk phase tends to sweep the surface film towards the rear of the bubble (see figure 1). There its escape is either prevented by its insolubility or

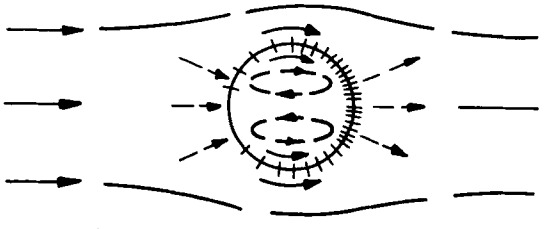

FIGURE 1. Surface film on a bubble in uniform flow.

impeded by the kinetics of the desorption process and/or diffusion in the bulk phase. Consequently, the movement of the surface film is slower than that of the main stream, and so velocity gradients normal to the boundary are produced. The resulting shear stresses tend to compress the film, causing a gradient of decreasing surface tension from front to rear of the surface. Because of the axial symmetry of the flow, the surface film 'locks' the surface, isolating the internal

fluid from the interfacial shear stresses which would otherwise cause internal circulation.

In flows which are not axially symmetrical, it will be shown that the presence of surfactants at a finite surface may cause steady circulatory velocities at the interface, so that part of the surface moves backwards against the general direction of flow of the main stream. Experimental investigations of two such flows are described in this paper. In one case the flow is amenable to analysis, and good agreement is obtained between the experimentally determined velocity field and the theoretical solution derived from a simple model of the surface film in which its solubility, compressibility and resistance to shear are all neglected.

2. Laminar shear flow past a hemispherical bubble

2.1. *Experimental methods*

During an investigation of vapour-bubble nucleation in forced-convection heat-transfer, the flow pattern near a stationary hemispherical air bubble on a wall bounding a laminar shear flow of water was investigated experimentally, using

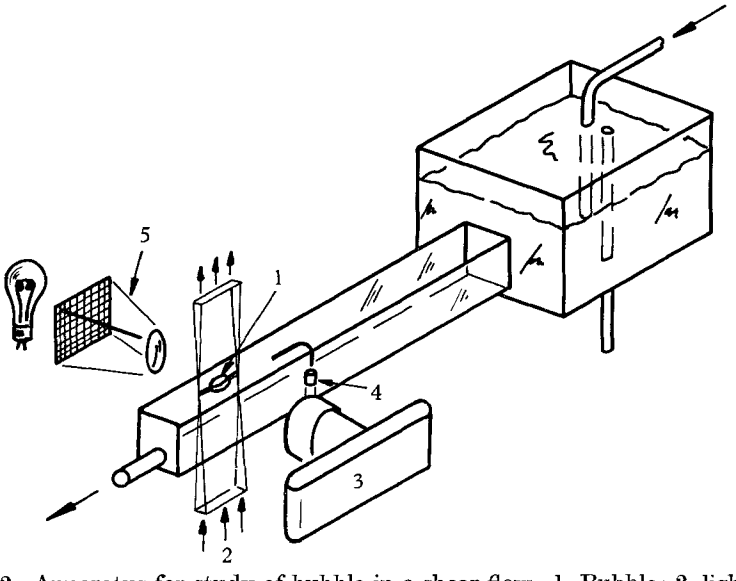

FIGURE 2. Apparatus for study of bubble in a shear flow. 1, Bubble; 2, light beam; 3, 35 mm camera; 4, dye injection; 5, reference grid projection system.

a dye filament and suspended aluminium powder to render the flow streamlines visible.

The air bubble rested against the top surface of a Perspex duct of 1 in. square cross-section which was supplied with tap-water from a constant-head tank (figure 2). Nearly all experiments were performed on bubbles of approximately 0·15 in. diameter, since this was the largest size for which there was negligible departure from spherical shape due to buoyancy forces. The bubble showed no tendency to move downstream at the low rates of flow used in the channel, presumably being restrained by a slight difference in the contact angle with the Perspex wall at its front and rear, although this was not detectable in photo-

graphs. The flow through the channel was laminar with a fully developed velocity profile at the bubble position, so that the flow approaching the bubble approximated to a linear shear flow (figure 3).

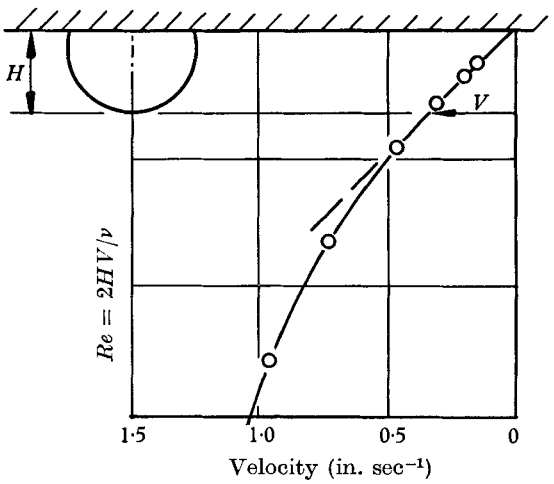

FIGURE 3. Definition of bubble Reynolds number.

A dye filament was introduced through an adjustable capillary tube 2 in. upstream from the bubble to show the general pattern of the three-dimensional flow near the bubble. More detailed investigations of the flow on the central plane of symmetry were made by photographing aluminium particles suspended in the water and illuminated by a thin sheet of light from a mercury vapour lamp flashing at 100 c/s. A special optical system combining spherical and cylindrical lenses, described by Kenning (1964), was used to restrict the zone of illumination to a thin vertical beam which for a distance of 0·3 in. had a constant horizontal cross-section measuring 0·010 in. by 0·8 in. The flow was photographed in a direction perpendicular to the light beam using a 35 mm camera fitted with a lens-extension tube. Velocities were obtained by measuring the interrupted traces of individual particles. At fluid velocities above 0·5 in./sec, the flashing of the lamp at 100 c/s gave traces of convenient length, but for measurements in regions of low velocity near the wall it was necessary to interrupt the light beam at about 10 c/s by a rotating shutter. On each photograph the image of an illuminated reference grid was projected on to the central plane of the bubble (figure 2), thus outlining the bubble and providing a scale of length.

2.2. *Experimental observations*

A Reynolds number Re, for the flow was defined in terms of the maximum distance of the bubble surface from the wall and the velocity in the approaching stream at this distance (figure 3).

The general pattern of the three-dimensional flow at Re about 30 is sketched in figure 4 from visual observations of the dye filament. Photographs of the flow on the central plane of symmetry are reproduced in figures 5–9 (plates 1 and 2). Figure 5 (plate 1) shows a bubble at $Re = 2$. The water velocities were very low in

this particular case and there is some distortion of the streamlines due to the finite sinking speed of the aluminium particles. Figure 6 (plate 1) shows a bubble at $Re = 250$, and figure 7 (plate 1) shows a large, and consequently distorted, bubble at $Re = 46$. Figures 8 and 9 (plate 2) show respectively a bubble and a solid obstacle, both at $Re = 30$.

At high Re, a large vortex formed ahead of the bubble, with its axis curving round the sides of the bubble and away downstream in a horseshoe shape. Similar vortices near solid obstacles in laminar boundary layers were described by Gregory & Walker (1950) and Thwaites (1960). The vortex became smaller

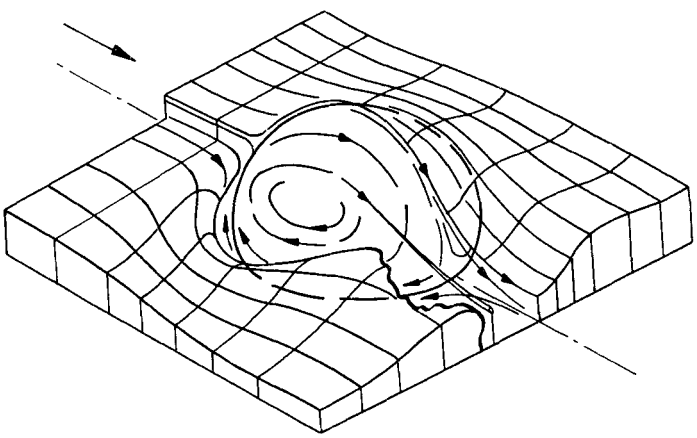

FIGURE 4. Impression of flow past bubble at $Re = 30$.

at lower Re and was indiscernible at $Re < 2$. The size of the vortex was measured by the initial distance from the wall to the 'dividing stream-line', namely the one separating the fluid on the central plane which entered the vortex, turning towards the wall, and that which flowed away from the wall over the tip of the bubble. This distance, expressed as a fraction of the bubble height, is plotted against Re in figure 10.

Another feature of the flow, with which this paper is primarily concerned, was a steady circulation in the bubble surface. Near the point on the bubble furthest from the wall (hereafter called the 'tip' of the bubble), the surface moved in the direction of the main stream, but near the wall the surface moved from the rear towards the front of the bubble, so that stagnation points existed on each shoulder of the bubble. The motion of the water adjacent to the bubble surface could be followed by eye when a dye filament was directed along the dividing streamline. Some dye entered the vortex, while the rest moved slowly away from the wall over the tip of the bubble and then in towards the wall at the rear. It then moved back along the base of the bubble close to the wall, inside the horseshoe vortex, until it reached the front of the bubble, where it finally moved away from the wall again over the bubble surface. Precise details of the flow very close to the wall at the front of the bubble could not be observed. The entire surface of the bubble became tinted with dye, and two thin filaments left the bubble near the shoulder stagnation points. The whole surface of the bubble appeared to be washed by fluid which had approached along the dividing streamline.

Figure 7 shows clearly the way fluid is drawn towards the wall near the rear of the bubble. It then flows near the wall to the front of the bubble, where it interacts with the upstream vortex; streamlines on the edge of the vortex which have started to turn towards the wall are deflected back over the tip of the bubble.

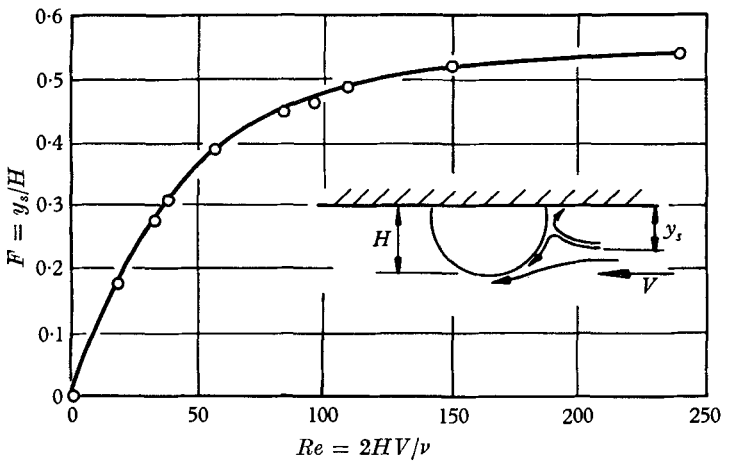

FIGURE 10. Distance of dividing streamline from wall.

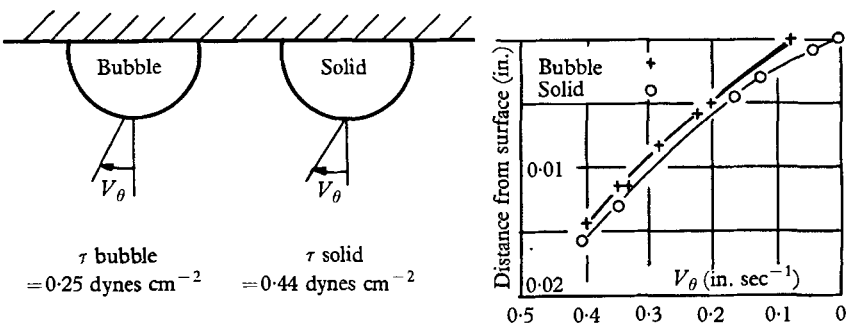

FIGURE 11. Velocity gradients at bubble and solid surfaces, $Re = 30$.

One consequence of the circulation was to delay separation of the flow into a wake behind the bubble. The flow past a bubble at $Re = 30$ (figure 8) was compared with the flow past a solid obstacle of similar shape also at $Re = 30$ (figure 9). The solid showed a separated wake region, but separation occurred behind the bubble only at much higher values of Re as in figure 6 for example. No reversed flow was observed along the sides of the solid, and the dividing streamline ended in a stagnation point on the front surface. The upstream vortex was slightly larger than that for a bubble at the same Re, possibly because of the absence of circulation-induced flow away from the wall at the leading edge. The surface shear stresses at the tip of the bubble and the solid were calculated from the velocity measurements (figure 11). Despite its mobility, the shear stress at the bubble surface was nearly 60 % of that at the solid surface.

It was realized that the presence of a surface film might account for these phenomena, so the surface tension of the tapwater was measured. It varied from day to day between approximate limits of 55 and 65 dyn cm^{-1} at 20 °C, indicating

that a soluble surfactant of unknown constitution was certainly present. Since no special precautions had been taken to degrease the apparatus, it would also have been possible for insoluble surfactants to migrate along the channel wall to the bubble surface.

2.3. *Discussion of surface circulation*

In respect of this complicated three-dimensional flow, it might be argued that the surface circulation could be a consequence of the secondary-flow pattern or of the internal circulation of the gas inside the bubble. However, no reversed flow was observed near the surface of the solid hemisphere, and the measured shear stress at the bubble surface was too large to be accounted for by the viscosity of the internal gas: for uniform flow at low Reynolds numbers Landau & Lifshitz (1959) give the theoretical ratio of shear stresses on fluid and solid spheres as only 1 : 101 for a gas-to-liquid viscosity ratio of 1 : 100, and the ratio in a shear

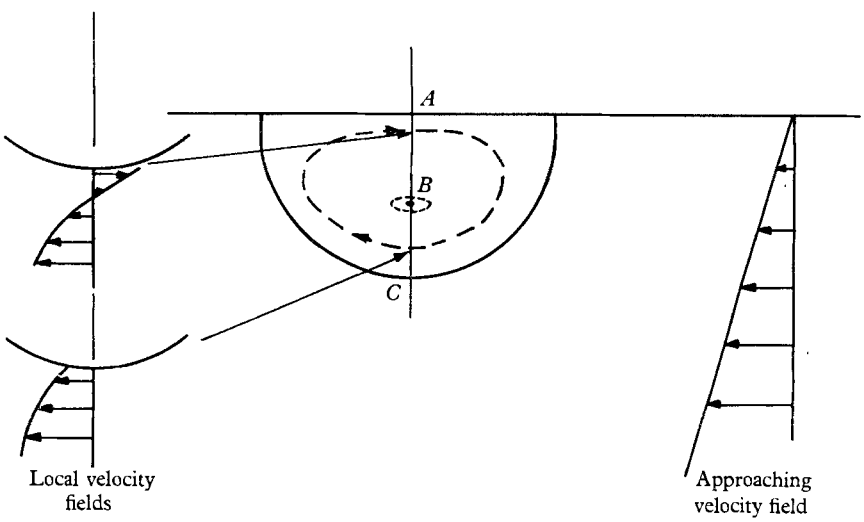

FIGURE 12. Production of surface circulation.

flow might be expected to be of the same order. Again by analogy with bubbles in uniform flow, the large surface shear stresses suggest that the bubble was covered by a mono-molecular film of surface-active agent, which was either insoluble or had such a low diffusion coefficient that interchange of material between the liquid phase and the surface could only take place very slowly. The surface tension measurements showed that such surfactant could well have been present.

A surface film would be subject to equations of motion and continuity additional to those of the bulk fluid. While analysis is deferred until § 3.2, it can be shown qualitatively that the presence of a film would account for the observed surface circulation. The relatively large stream velocities near the tip of the bubble tend to sweep the surface film downstream towards the rear of the bubble, but this effect is smaller near the channel wall where the stream velocities are low. If the film cannot escape from the surface at the rear of the bubble, it must return upstream along the surface near the wall. Circulation of the surface film thus builds up, reducing velocity gradients normal to the surface at the tip of the

bubble and increasing those near the wall, until the shear forces acting on different parts of any closed loop drawn on the surface are balanced (see figure 12). If the solubility of the film is negligible and it is further assumed to be incompressible and of constant (monomolecular) thickness, continuity requires that the flow across AB should equal that across BC. While observation of the bubble gave the impression that this was so, no quantitative measurement of surface velocities was possible other than on the plane of symmetry of the flow. It was therefore decided to devise a flow demonstrating surface circulation which would be easier to observe and analyse than the flow past a bubble, so that boundary conditions at the surface could be examined in more detail.

3. Open channel flow with surface barriers

3.1. *Experimental study*

Surface circulation is to be expected when there is non-uniform flow of liquid containing surfactant past a finite interface with another fluid. These conditions were obtained by a modification to the steady laminar flow of tap-water along

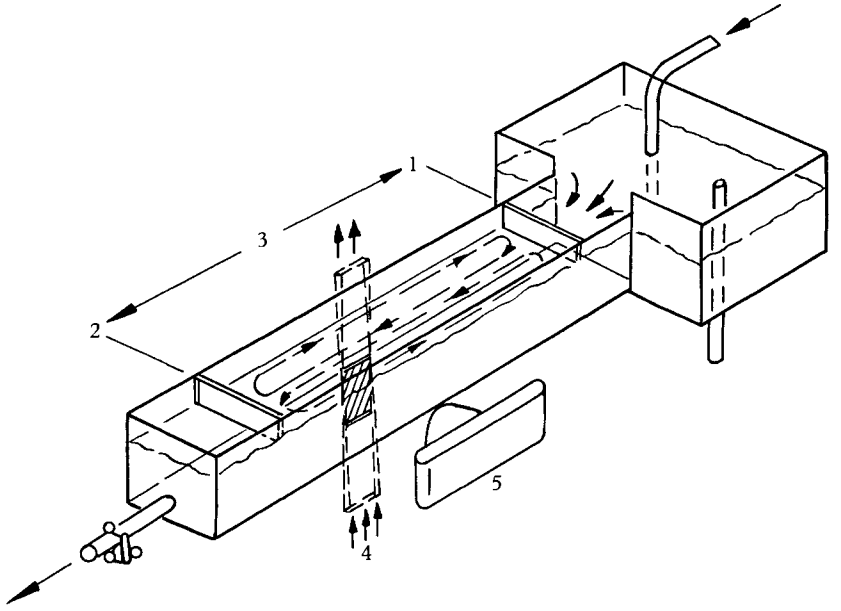

FIGURE 13. Open-channel apparatus. 1, Upstream barrier; 2, downstream barrier; 3, circulating zone; 4, light beam; 5, camera.

an open rectangular channel. Transverse barriers were placed near the ends of the channel so that they just touched the water surface from above (figure 13). The barriers and the channel walls then defined a rectangular surface zone in which circulation occurred.

The Perspex channel was 48 in. long by 0·96 in. wide. Tapwater was supplied from a constant-head tank, and the channel slope was carefully adjusted to maintain a constant water depth of 0·53 in. The first barrier was placed 12 in. from the channel entrance, and there was a distance of 30 in. between barriers.

Fluid velocities in the region between the barriers were everywhere parallel with the channel axis, except for lengths of about 2 in. near each barrier. Velocities were measured by photographing the tracks of aluminium particles sus-

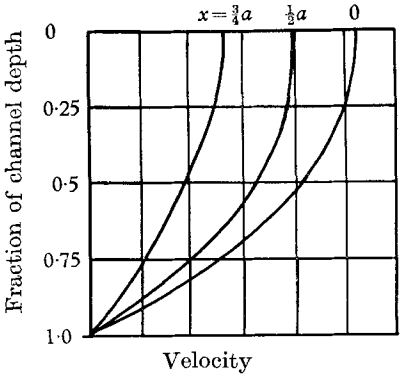

FIGURE 14. Open-channel velocity distributions in absence of surfactant (Straub *et al.* 1956).

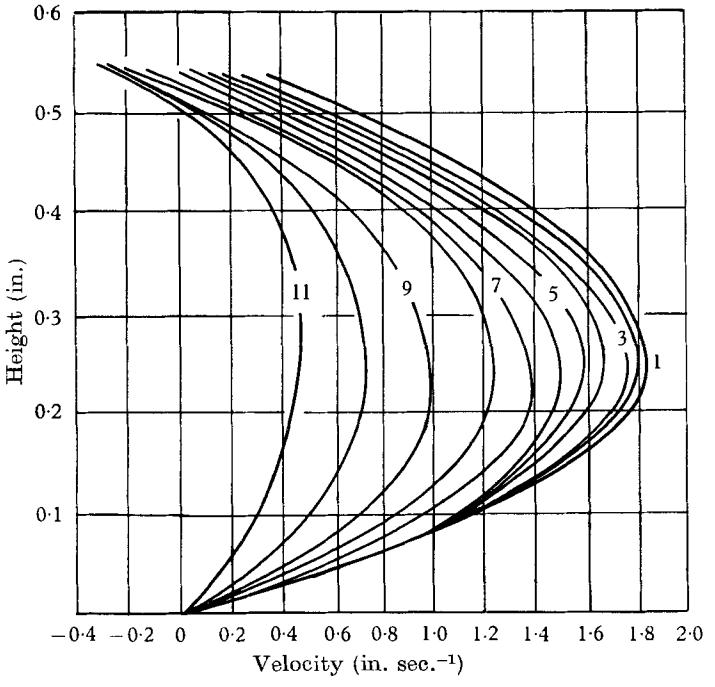

FIGURE 15. Experimental velocity distributions for tap-water.

Position ...	1	2	3	4	5	6	7	8	9	10	11
x/a	0	0·17	0·25	0·33	0·42	0·48	0·58	0·67	0·75	0·83	0·92

pended in the water, as in the bubble study. By traversing the light beam across the channel, it was possible to measure velocity distributions on a series of vertical planes at different distances from the channel centre-line. All measurements were made 8 in. upstream from the second barrier, in the region of parallel flow.

In the absence of surface-active agents, the shear stress at the free surface should be negligibly small, so that the established velocity profile in laminar flow is that given by Straub *et al.* (1956) and sketched in figure 14, with the maximum velocity on any vertical plane occurring at the free surface. In the present experiments with tap-water, a completely different flow pattern was observed, as shown in figure 15. Large velocity gradients existed at the free surface, so that the positions of maximum velocity lay, not at the surface, but at approximately mid-depth of the channel. A steady circulation of the form shown in figure 16 existed over the entire surface between the barriers, so that there was

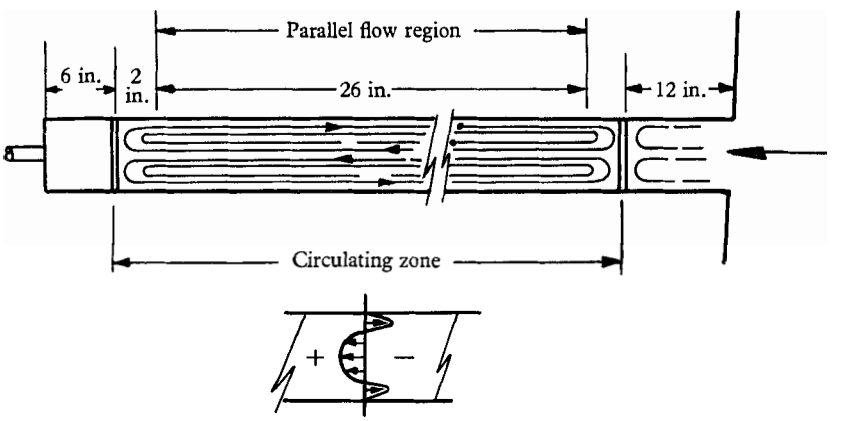

FIGURE 16. Surface circulation in open channel.

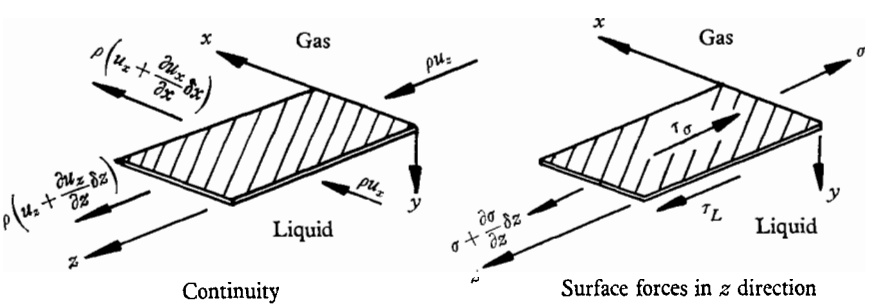

FIGURE 17. Plane surface element.

little or no net flow of surface along the channel. The qualitative explanation of this circulation is similar to that for shear flow past a bubble. The water surface between the barriers is covered by a virtually insoluble monomolecular film of surfactant which is subjected to shear stresses by the underlying water flow. In the middle of the channel the general stream velocity is high, so the shear stress at the surface is high. Near the walls the stream velocity is lower, and the shear stress tends to be lower. The surface therefore flows upstream near the walls. It was demonstrated that the circulation was indeed due to a surface film by applying to the surface near the downstream barrier a capillary tube attached to a suction pump. If the tip of the tube was slightly immersed so that it drew water from the bulk liquid immediately below the surface but not from the surface

itself, the surface circulation was unaffected. If, however, the pump was arranged to draw water from the surface, the circulation disappeared immediately and was replaced by a flow with zero velocity gradient at the free surface. Removal of the surface film by suction destroyed the continuity condition which otherwise caused the reversed surface flow near the walls.

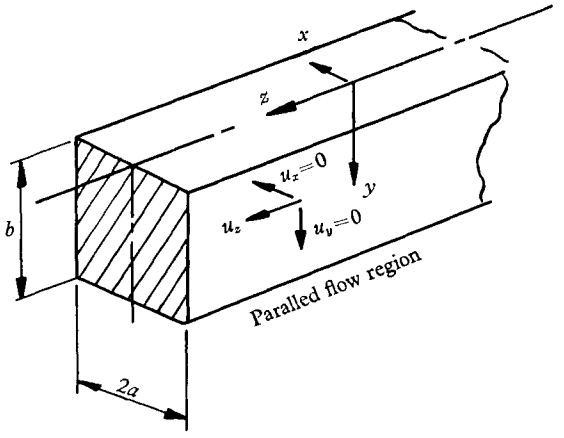

FIGURE 18. Open-channel flow, region for analysis.

3·2. *Theoretical analysis*

A simple model is set up to represent the chief aspects of the flow régime described above. Boundary conditions are established for a plane interface between a gas and an incompressible liquid in steady motion in the presence of surface-active material. It is assumed that the surface-active agent forms at the interface an insoluble, incompressible monomolecular film, which exhibits negligible resistance to shear, i.e. zero surface viscosity. The validity of these assumptions is discussed briefly in §4.

Considering an element of the surface lying in the (x, z)-plane, as defined in figure 17, the condition on the velocity (u_x, u_y, u_z) for the continuity of the film may be written in either of the equivalent forms

$$\frac{\partial u_x}{\partial x}+\frac{\partial u_z}{\partial z}=0 \quad \text{at} \quad y=0, \tag{1}$$

or

$$\oint u_n dl = 0 \quad \text{at} \quad y=0. \tag{2}$$

Also, if there is no slip between the film and the adjacent bulk phase, equation (1) may be subtracted from the continuity equation for that phase, to give

$$\frac{\partial u_y}{\partial y}=0 \quad \text{at} \quad y=0. \tag{3}$$

In the absence of surface viscosity and neglecting the inertia of the film, the force balance on the film shows that the viscous shear stress acting on the film in any direction from the bulk phases must be balanced by a gradient of surface tension in that direction. If shear stresses in the gas are negligible, this implies

that the shear stresses applied by the liquid to the surface are irrotational. From this, a boundary condition for the liquid velocity is readily derived (Kenning 1964):

$$\frac{\partial}{\partial y}\{(\text{curl}\,\mathbf{u})_y\} = 0 \quad \text{at} \quad y = 0. \tag{4}$$

Since finding the condition in this form, the writers' attention has been drawn to the more general form given by Scriven & Sternling (1964, equation (6)).

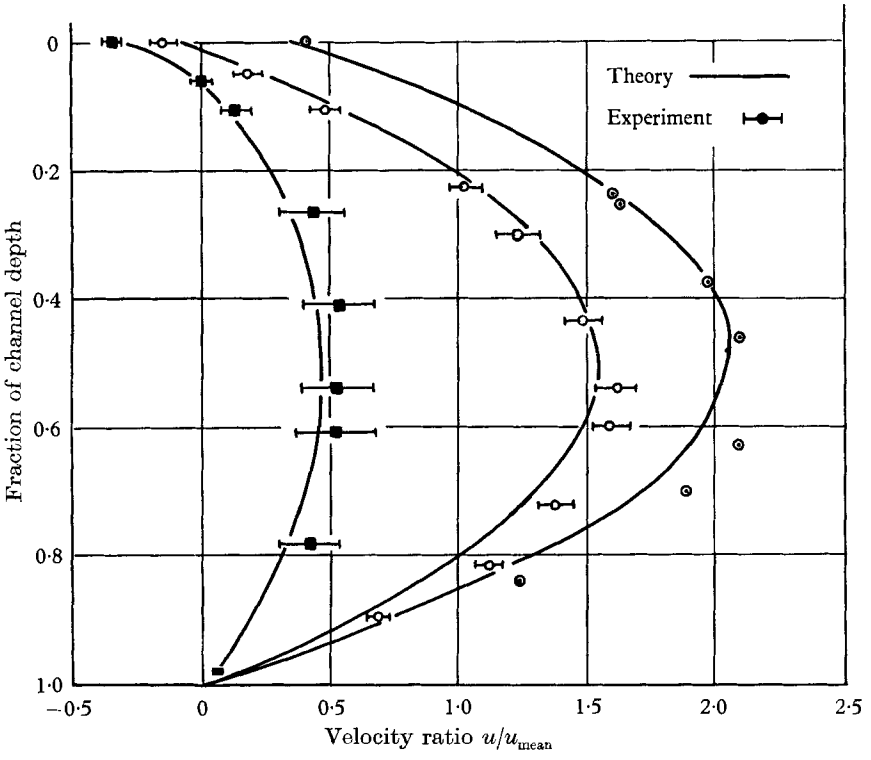

FIGURE 19. Comparison of theoretical and experimental velocity distributions in open channel: ⊙, $x/a = 0$; ○, $x/a = 0{\cdot}58$; ■, $x/a = 0{\cdot}92$.

These boundary conditions are now applied to the region of the channel flow between the barriers (figure 19). Apart from short lengths near the barriers, it is assumed that

$$u_x = u_y = 0 \quad \text{and} \quad u_z = f(x, y). \tag{5}$$

In this region of steady parallel flow, the Navier–Stokes equations for the liquid reduce to

$$\frac{\partial^2 u_z}{\partial x^2} + \frac{\partial^2 u_z}{\partial y^2} = -g\frac{S}{\nu}, \tag{6}$$

where S is the slope of the channel and ν is the kinematic viscosity of the liquid. The continuity equation for the liquid is satisfied identically, and the continuity equation for the surface film (1) is also satisfied identically, but it is necessary to consider the effect of the downstream barrier on the motion of the surface film. That is most conveniently done by applying equation (2) to a path in the interface defined by the downstream barrier, the channel walls and the plane

$z = 0$, where the origin has been taken in the region of steady parallel flow. This yields

$$\int_{-a}^{+a} u_z dx = 0 \quad \text{at} \quad y = 0. \tag{7}$$

The second boundary condition (4) yields

$$\frac{\partial^2 u_z}{\partial x \partial y} = 0 \quad \text{at} \quad y = 0. \tag{8}$$

In addition we have

$$u_z = 0 \quad \text{at} \quad x = \pm a, \tag{9}$$

$$u_z = 0 \quad \text{at} \quad y = b. \tag{10}$$

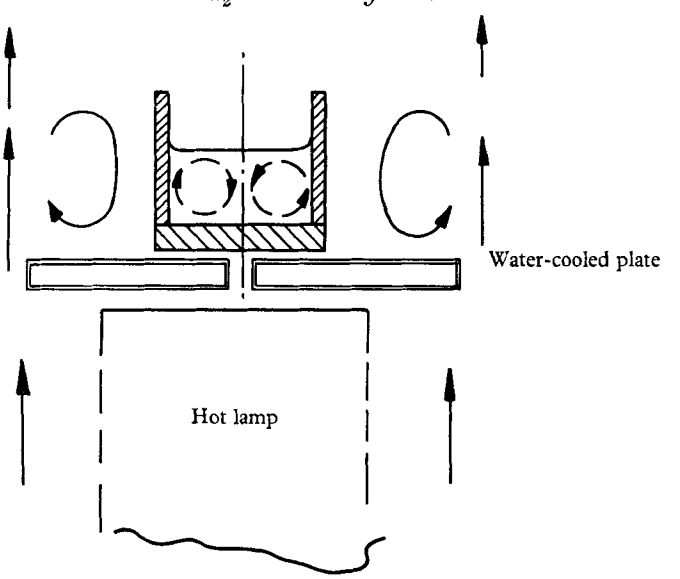

FIGURE 20. Secondary circulation in open channel.

In this simple configuration of steady parallel flow, condition (8) can be established without recourse to (4), as shown by Landau & Lifshitz (1959, §62), quoting from a paper by Levich.

Equation (6) with the boundary conditions (7) to (10) was solved for u_z in series form, as shown in the Appendix, and also by two approximate methods. One approximate method employed a relaxation net, using trial and error to satisfy (7) and (8). The other employed flow nets, constructed graphically. The ratio a/b was taken to be 0·9, to permit comparison with experimental results available for that configuration. Typical velocity distributions given by the approximate solutions and the corresponding experimental measurements are plotted in figure 19. The possible errors in the experimental values due to the finite width of the light beam (0·010 in.) are indicated, becoming significant near the walls where $\partial u_z/\partial x$ was large. The experimental positions of maximum velocity lie rather closer to the bottom of the channel than the theoretical positions. This may have been due to a very slow circulation in the bulk flow (figure 20), caused by heating of the channel walls by hot air rising from the light source, since a slight circulation of this form was still evident when there was no flow of water through the channel.

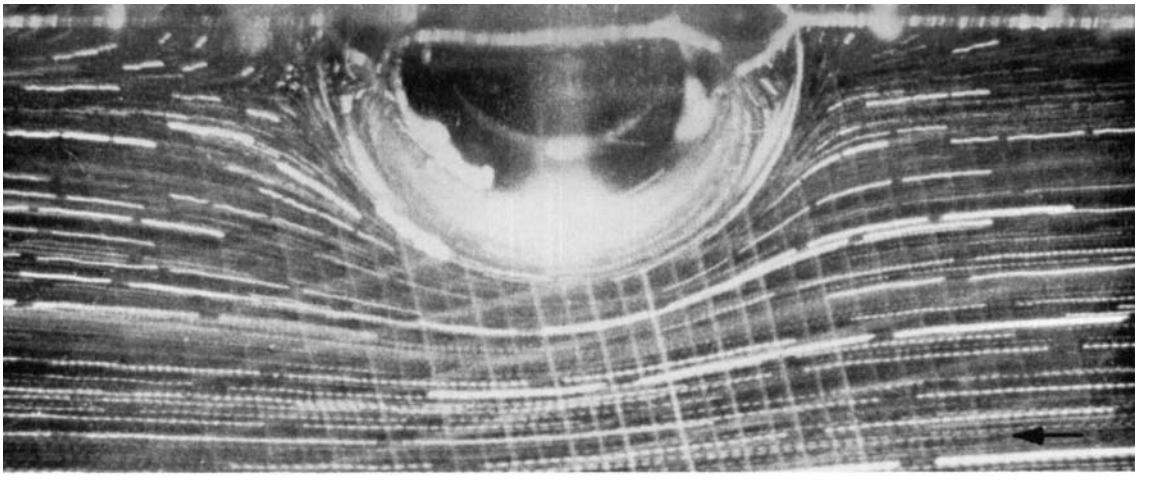

FIGURE 5. Photograph of flow past bubble at $Re = 2$.

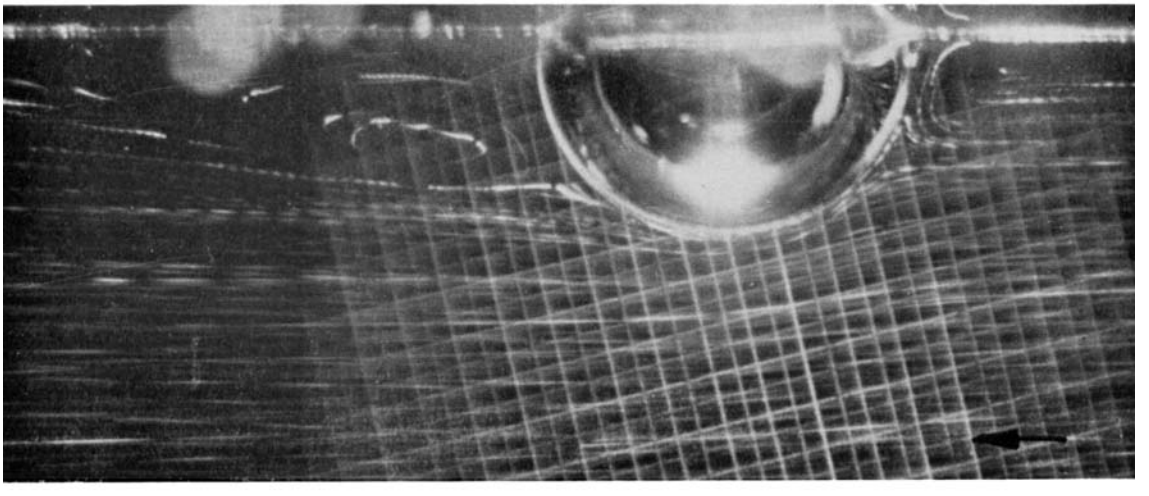

FIGURE 6. Bubble at $Re = 250$.

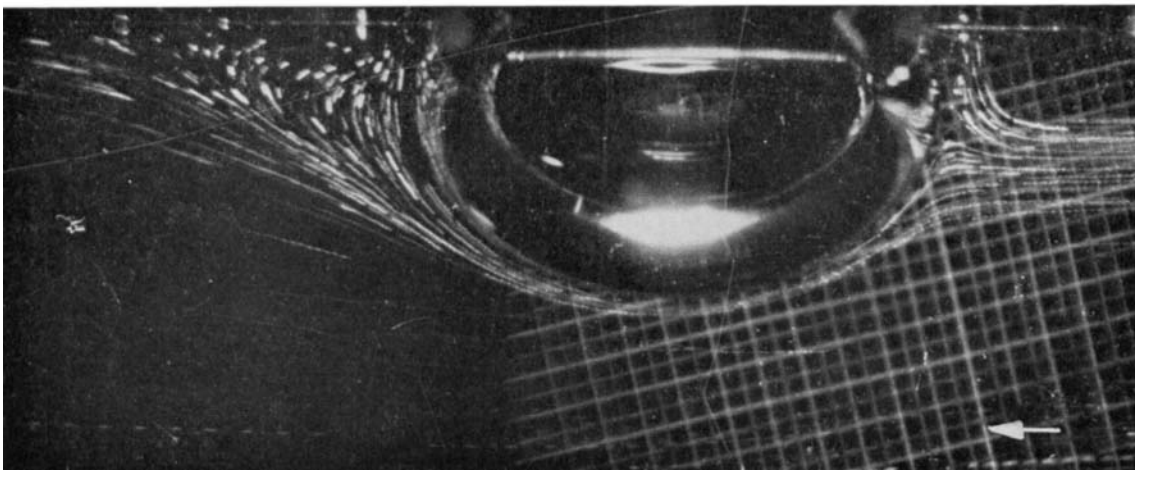

FIGURE 7. Distorted bubble at $Re = 46$.

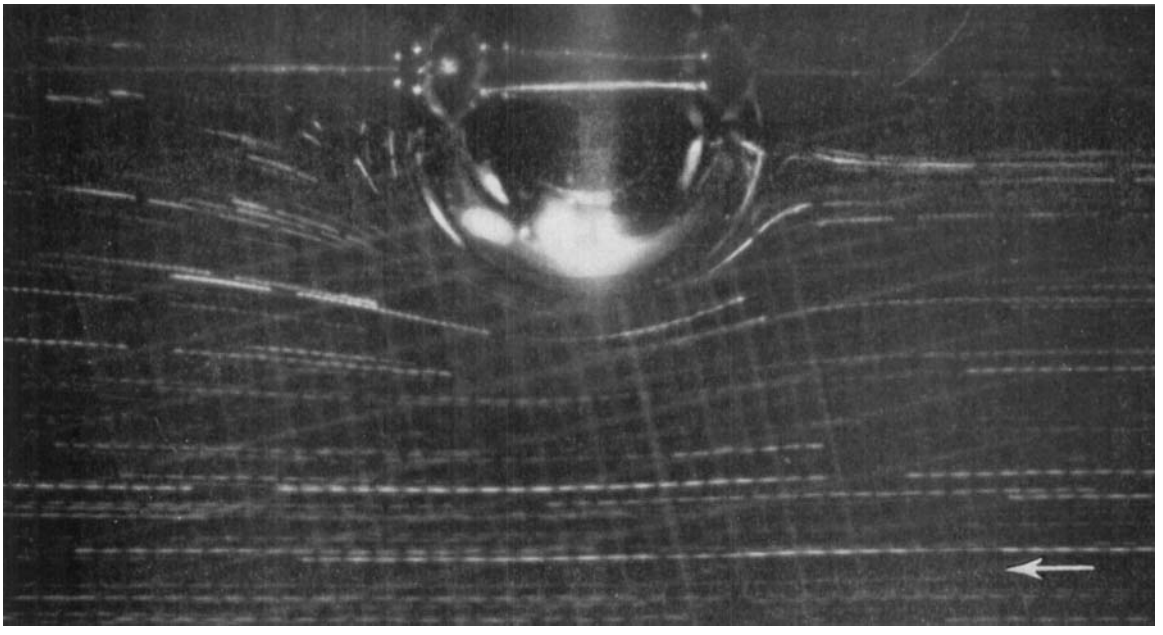

FIGURE 8. Bubble at $Re = 30$.

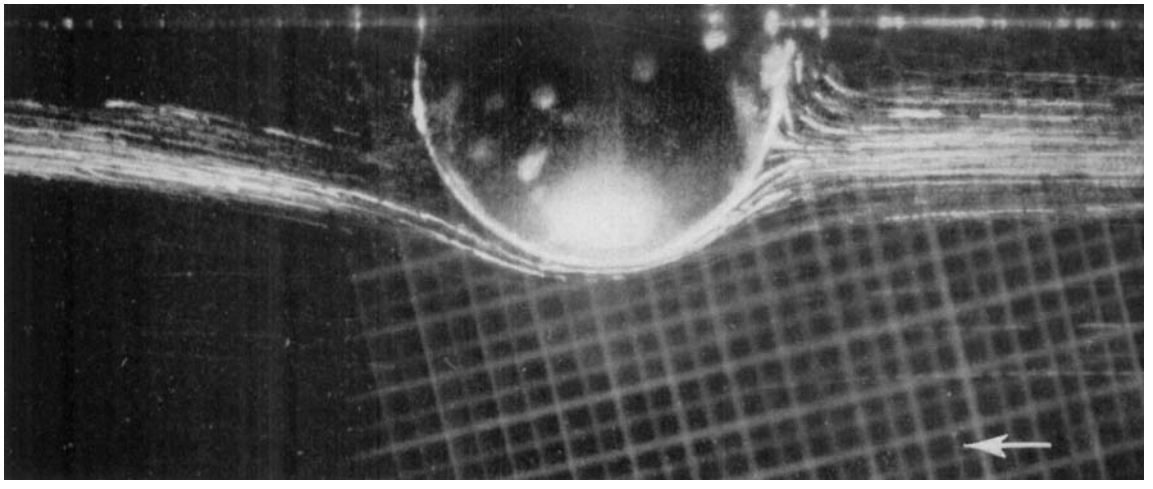

FIGURE 9. Solid at $Re = 30$.

4. Discussion

The agreement between experiment and theory for the open-channel flow suggests that the explanation advanced for the circulation of the surface of a hemispherical bubble in a shear flow was correct. Similar surface-circulation patterns may be expected whenever there is non-uniform flow of liquid containing a surfactant past a finite fluid interface.

The boundary conditions for the liquid phase derived by assuming that the surface film on tap-water was insoluble and incompressible were otherwise independent of the nature or amount of surfactant present. Where the effect of the gaseous phase could be ignored, the Reynolds number, together with the Froude and Weber numbers, remained the only parameters governing the liquid flow.

The assumptions concerning the nature of the surface film may not always be valid. The equations of state of insoluble surface films under static conditions, described by Adam (1941), show that the surface area per molecule of surfactant approaches a constant limiting value only at high values of the surface pressure (i.e. large surface-tension reduction). The solubility of the film may also be appreciable under certain conditions: by adding large amounts of commercial detergent (Quix), exceeding the critical micelle concentration, to the water in the open channel it was possible to produce a net surface flow downstream, although there was still some reversed flow near the walls. Similar treatment had no detectable effect on the circulation of the bubble surface, however. The resistance of surface films to shear deformation has been reviewed by Davies & Rideal (1961). For a given Reynolds number, surface viscosity becomes more important as the linear scale of the flow is reduced and would tend to inhibit surface circulation, giving a stagnant surface film.

This paper is based on part of the dissertation submitted to Cambridge University for the degree of Doctor of Philosophy by D. B. R. Kenning. The work was financed by the U.K. Atomic Energy Authority. The award of a U.K.A.E.A. Bursary to D. B. R. Kenning during 1960–63 is gratefully acknowledged.

Appendix

We need a solution in series form for

$$\nabla^2 u = -K,$$

with

$$\frac{\partial^2 u}{\partial x \partial y} = 0 \quad \text{on} \quad y = 0,$$

$$u = 0 \quad \text{on} \quad x = \pm a, \quad u = 0 \quad \text{on} \quad y = b,$$

also

$$\int_{-a}^{a} u\,dx = 0 \quad \text{on} \quad y = 0.$$

We first take the known solution in series form for

$$\nabla^2 u_1 = -K,$$

with

$$\frac{\partial u_1}{\partial y} = 0 \quad \text{on} \quad y = 0,$$

$$u_1 = 0 \quad \text{on} \quad x = \pm a, \quad u = 0 \quad \text{on} \quad y = b.$$

This is (Straub *et al.* 1956)

$$u_1 = \tfrac{1}{2}K(b^2-y^2)+\sum_{m=1}^{\infty} A_m \cosh\frac{m\pi x}{2b}\cos\frac{m\pi y}{2b},$$

where

$$A_m = -\frac{16Kb^2}{m^3\pi^3}\frac{\sin\frac{1}{2}(m\pi)}{\cosh(m\pi a/2b)}.$$

We then obtain the solution in series form for

$$\nabla^2 u_2 = 0,$$

with

$$\frac{\partial u_2}{\partial y} = 1 \quad \text{on} \quad y = 0,$$

$$u_2 = 0 \quad \text{on} \quad x = \pm a, \quad u_2 = 0 \quad \text{on} \quad y = b.$$

This is found to be

$$u_2 = \sum_{n=1}^{\infty} C_n \cos\frac{n\pi x}{2a}\sinh\frac{n\pi(b-y)}{2a},$$

where

$$C_n = -\frac{8a}{n^2\pi^2}\frac{\sin\frac{1}{2}(n\pi)}{\cosh(n\pi b/2a)}.$$

On $y = 0$, we have

$$\int_{-a}^{a} u_1 dx = Kab^2 - K\sum_{m=1}^{\infty}\frac{64b^3}{\pi^4 m^4}\tanh\frac{m\pi a}{2b}\sin\frac{m\pi}{2} = \phi, \quad \text{say},$$

and

$$\int_{-a}^{a} u_2 dx = -\sum_{n=1}^{\infty}\frac{32a^2}{\pi^3 n^3}\tanh\frac{n\pi b}{2a}\sin\frac{n\pi}{2} = \psi, \quad \text{say}.$$

The required solution is therefore

$$u = u_1 - \frac{\phi}{\psi}u_2.$$

REFERENCES

Adam, N. K. 1941 *The Physics and Chemistry of Surfaces.* Oxford University Press.

Davies, J. T. & Rideal, E. K. 1961 *Interfacial Phenomena.* New York: Academic Press.

Frumkin, A. & Levich, V. 1947 *Zh. Fiz. Khim.* **21**, 1183. (See also Levich, V. 1962 *Physico-chemical Hydrodynamics.* New Jersey: Prentice-Hall.)

Gardner, F. H. & Hale, A. R. 1953 *Chem. Engng Sci.* **2**, 157.

Gardner, F. H. & Skelland, A. H. P. 1951 *Trans. Inst. Chem. Engrs*, **29**, 315.

Gregory, N. & Walker, W. S. 1950 *Aero. Res. Counc., London, R & M* no. 2779.

Griffith, R. M. 1960 *Chem. Engng Sci.* **12**, 198.

Griffith, R. M. 1962 *Chem. Engng Sci.* **17**, 1057.

Kenning, D. B. R. 1964 Ph.D. Thesis, Cambridge University.

Landau, L. D. & Lifshitz, E. M. 1959 *Fluid Mechanics.* London: Pergamon Press.

Scriven, L. E. & Sternling, C. V. 1964 *J. Fluid Mech.* **19**, 321–40.

Straub, L. G., Silberman, E. & Nelson, H. C. 1956 *Proc. Amer. Soc. Civ. Engrs* **82**, *J. Engng Mech. Div.*, Paper no. 1031.

Thwaites, B. 1960 *Incompressible Aerodynamics.* Oxford University Press.

Note added at proof stage

Circulation patterns on the surface of an open-channel flow, similar to those described in this paper, have recently been reported by R. L. Merson & J. A. Quinn (1965 *J. Amer. Inst. Chem. Engrs*, **11**, 391).